Simultaneous Spectrum Sensing and Data Transmission for Multi-User MIMO Cognitive Radio Systems

Nikolaos I. Miridakis,* Theodoros A. Tsiftsis,‡ George C. Alexandropoulos,§ and Mérouane Debbah§
*Department of Computer Engineering, Piraeus University of Applied Sciences, 12244 Aegaleo, Greece
‡School of Engineering, Nazarbayev University, 010000 Astana, Kazakhstan
§Mathematical and Algorithmic Sciences Lab, France Research Center, Huawei Technologies Co. Ltd.
e-mails: nikozm@unipi.gr, theodoros.tsiftsis@nu.edu.kz, {george.alexandropoulos, merouane.debbah}@huawei.com

***Abstract*—We present a multi-user multiple-input multiple-output (MIMO) cognitive radio system consisting of a secondary receiver that deploys spatial multiplexing to decode signals from multiple secondary transmitters, under the presence of primary transmissions. The secondary receiver carries out minimum mean-squared error detection to decode the secondary data streams, while it performs spectrum sensing at the remaining signal to capture the potential presence of primary activity. Assuming Rayleigh fading as well as the realistic cases of channel fading time variation and channel estimation errors, we present novel closed-form expressions for important system measures, namely, the detection and false-alarm probabilities as well as the transmission power of the secondary nodes. The enclosed numerical results verify the accuracy of the presented analysis.**

***Index Terms*—Cognitive radio, detection probability, imperfect channel estimation, spatial multiplexing, spectrum sensing.**

I. Introduction

Spectrum sensing plays a key role in the performance of shared access networks by impacting the performance of both the primary and secondary networks. Several spectrum sensing approaches, that vary on the accomplished reliability of primary activity detection, have been proposed so far to preserve the transparency of cognitive radio (CR) networks. These approaches can be categorized into the following two main types: *i*) quiet [1]; and *ii*) active [2].

The conventional approach for spectrum sensing is the quiet type, according to which each potential cognitive transmitter first senses the spectrum for a fixed-time duration, and then transmits its data in the remaining time, if it senses the channel as idle. The main problem with this sensing type is the capacity reduction for the secondary data transmission within a given frame duration. In order to overcome this problem, the more sophisticated active sensing type has been proposed [2]–[4]. In particular, a simultaneous spectrum sensing and data transmission approach was proposed in [3], where the receiver first cancels the secondary data using interference cancellation, and then, senses the remaining signal for the presence or absence of a primary activity. Other active sensing techniques for multi-user cognitive systems were proposed in [2] and [4]. In both studies, it was assumed that some secondary nodes transmit, while others perform spectrum sensing. In the case of a primary signal detection, the latter nodes inform the former ones about the primary activity and request to them to stop their transmissions. Nevertheless, several problems arise by following these two approaches; more spectrum resources are required because of the signaling overhead caused by the informing process whereas, extra power resources are consumed from the sensing nodes during spectrum sensing and because of transmitting their sensing reports.

In this paper, a new simultaneous (active) spectrum sensing and data transmission approach for multi-user multiple-input multiple-output (MIMO) CR networks is presented. The spectrum sensing is performed at the multi-antenna secondary receiver upon the signal reception from multiple secondary single-antenna transmitters. The spatial multiplexing mode of operation is adopted, for the first time, where all the potential secondary transmitters send their data streams simultaneously in a given frame duration. Overall, the main benefits of the proposed approach are threefold: (a) the sensing and data transmission time are both optimal since they coincide with the entire frame duration. Thus, the accuracy of the performance of primary activity detection is further improved. In addition, spectrum sensing is performed by the different transmitters (i.e., by nodes that are sufficiently separated in terms of transmission wavelengths), and thus, robust enough. Besides, the spatial multiplexing mode of operation further enhances the aggregate sum-capacity of the network; (b) an efficient tradeoff between sensing time and data transmission time, and its relevant computation is no longer an issue; and (c) the inter-user interference problem is effectively mitigated, since all antennas at the receiver are used first for signal detection/decoding for the secondary data and then for spectrum sensing in the same frame duration.

Notation: Vectors and matrices are represented by lowercase and uppercase bold typeface letters, respectively. Also, $\mathbf{X}^{-1}$ is the inverse of $\mathbf{X}$ and $\mathbf{x}_i$ denotes the ith coefficient of $\mathbf{x}$. A diagonal matrix with entries $x_1, \ldots, x_n$ is defined as $\mathrm{diag}\{x_i\}_{i=1}^{n}$. The superscripts $(\cdot)^T$ and $(\cdot)^{\mathcal{H}}$ denote transposition and Hermitian transposition, respectively, $\|\cdot\|$ corresponds to the vector Euclidean norm, while $|\cdot|$ represents absolute (scalar) value. In addition, $\mathbf{I}_v$ stands for the $v \times v$ identity

matrix, $\mathbb{E}[\cdot]$ is the expectation operator, $\overset{\text{d}}{=}$ represents equality in probability distributions, and $\Pr[\cdot]$ returns probability. Also, $f_X(\cdot)$ and $F_X(\cdot)$ represent the probability density function (PDF) and cumulative distribution function (CDF) of the random variable (RV) X, respectively. Complex-valued Gaussian RVs with mean μ and variance σ^2, while chi-squared RVs with v degrees-of-freedom are denoted, respectively, as $\mathcal{CN}(\mu, \sigma^2)$ and $\mathcal{X}^2_{2v}$. Furthermore, $\Gamma(a) \triangleq (a-1)!$ (with $a \in \mathbb{N}^+$) denotes the Gamma function [5, Eq. (8.310.1)], while $\Gamma(\cdot, \cdot)$ is the upper incomplete Gamma function [5, Eq. (8.350.2)]. Further, $J_0(\cdot)$ represents the zeroth-order Bessel function of the first kind [5, Eq. (8.441.1)], ${}_1F_1(\cdot, \cdot; \cdot)$ denotes the Kummer's confluent hypergeometric function [5, Eq. (9.210.1)], and $Q_\nu(\cdot, \cdot)$ is the generalized νth order Marcum-Q function [6].

II. System Model

We consider a multi-user MIMO secondary communication system, which is consisted of m_c single-antenna cognitive transmitters and a receiver equipped with $N \geq m_c$ antennas operating under the presence of m_p single-antenna primary nodes. Notice that, although $N \geq m_c$ is a necessary condition in order to capture the available degrees-of-freedom during the detection of the independent data streams from the cognitive transmitting nodes, it holds that $N \lesseqgtr (m_p + m_c)$. Moreover, independent and non-identically distributed Rayleigh flat fading channels are assumed, reflecting non-equal distances among the involved nodes with respect to the receiver; this is an appropriate condition for practical applications. The spatial multiplexing mode of operation is implemented in the secondary system, where m_c independent data streams are simultaneously transmitted by the corresponding secondary nodes. A suboptimal yet quite efficient detection scheme is adopted at the secondary receiver, the so-called linear minimum mean-squared error (MMSE).

Using the definition $M \triangleq m_p + m_c$, the received signal at the nth sample time instance reads as

$$\mathbf{y}[n] = \hat{\mathbf{H}}[n]\mathbf{s}[n] + \mathbf{w}[n], \tag{1}$$

where $\mathbf{y}[n] \in \mathbb{C}^{N\times 1}$, $\hat{\mathbf{H}}[n] \in \mathbb{C}^{N\times M}$, $\mathbf{s}[n] \in \mathbb{C}^{M\times 1}$, and $\mathbf{w}[n] \in \mathbb{C}^{N\times 1}$ denote the received signal, the estimated channel matrix, the transmitted signal, and the additive white Gaussian noise (AWGN), respectively. It holds that $\mathbf{w} \overset{\text{d}}{=} \mathcal{CN}(\mathbf{0}, N_0\mathbf{I}_N)$ with N_0 denoting the AWGN variance and $\mathbf{s} = [s_1, \ldots, s_{m_p}, s_1, \ldots, s_{m_c}]^T$ with $\mathbb{E}[\mathbf{s}\mathbf{s}^{\mathcal{H}}] = \mathbf{I}_M$. In addition, $\hat{\mathbf{H}} = [\hat{\mathbf{h}}_1, \ldots, \hat{\mathbf{h}}_{m_p}, \hat{\mathbf{h}}_1, \ldots, \hat{\mathbf{h}}_{m_c}]$, whereas $\hat{\mathbf{h}}_i \overset{\text{d}}{=} \mathcal{CN}(\mathbf{0}, \beta_i\mathbf{I}_N)$, for $1 \leq i \leq M$, with $\beta_i \triangleq p_i/(d_i^{\omega_i})$, where p_i, d_i, and ω_i correspond to the signal power, normalized estimated distance (with a reference distance equal to 1km) from the receiver, and path-loss exponent of the ith transmitter (secondary or primary), respectively.

A. Protocol Description

The following three main phases, that are periodically alternating, constitute the mode of operation of the proposed multi-user MIMO CR system: the *training*, *data transmission*, and *spectrum sensing* phases.

During the training phase, all the involved nodes (i.e., primary and secondary transmitters) broadcast certain (orthogonal) pilot signals. The secondary receiver monitors the available spectrum resources in order to acquire the instantaneous channel gains from all the active transmit nodes (both primary and secondary). Meanwhile, all the secondary transmitters also monitor the channel in order to acquire the channel gains between the primary transmitters and themselves. This occurs in order to appropriately modify their power, which will be used for potential transmission in the subsequent data transmission phase. It is assumed that the channel remains constant during this phase. However, its status may change in subsequent time instances.

After the training phase, the system enters the data phase, where the secondary nodes stay inactive for one symbol time duration. During this time period, the secondary receiver senses the spectrum so as to capture the presence of a primary communication activity or not. In the former case, no transmission activity is performed by the secondary transmitters (lack of triggering from the secondary receiver in this case is interpreted as a busy spectrum notification to all the transmitters). This procedure is repeated in every subsequent symbol time duration, until the receiver senses the spectrum idle. In the latter case, the receiver broadcasts a certain probe message in order to initiate the secondary transmission(s). Hence, in the next symbol time instance, all active secondary transmitters may simultaneously send their data streams. Upon the overall signal reception, MMSE detection is performed at the secondary receiver and all data streams are decoded concurrently.

The spectrum sensing phase takes place after the removal of all secondary signals from the received signal. This happens within the same symbol time instance, where the receiver monitors the remaining signal for the presence of a potential primary activity. If the remaining signal is sensed idle (i.e., only the presence of noise), the same procedure keeps on (i.e., data transmission and spectrum sensing phases), until the next training phase. If at least one primary signal is detected at the remaining signal, then the receiver immediately broadcasts another certain message in order to coarsely finalize all the secondary transmissions.

B. Training Phase: Channel Estimation

To perform channel estimation during this phase, M orthogonal pilot sequences (i.e., unique spatial signal signatures) of length M symbols are assigned to the primary and secondary nodes. Then, the received pilot signal can be expressed as

$$\mathbf{Y}_{\text{tr}}[n] = \mathbf{H}_{\text{tr}}[n]\mathbf{\Psi} + \mathbf{W}_{\text{tr}}[n], \tag{2}$$

where $\mathbf{Y}_{\text{tr}}[n] \in \mathbb{C}^{N\times M}$, $\mathbf{H}_{\text{tr}}[n] \in \mathbb{C}^{N\times M}$, $\mathbf{\Psi} \in \mathbb{C}^{M\times M}$, and $\mathbf{W}_{\text{tr}}[n] \in \mathbb{C}^{N\times M}$ denote the received signal, the channel matrix, the transmitted pilot signals, and AWGN, respectively, all during the training phase. Also, the pilot signals are normalized in order to $\mathbb{E}[\mathbf{\Psi}\mathbf{\Psi}^{\mathcal{H}}] = \mathbf{I}_M$.

The MMSE estimate of $\mathbf{h}_i[n]$, $1 \leq i \leq M$, is given by [7, Eq. (10)] $\hat{\mathbf{h}}_i[n] = \beta_i(N_0 + \sum_{j=1}^{M}\beta_j)^{-1}\mathbf{I}_N(\sum_{j=1}^{M}\mathbf{h}_j[n] +$

$\mathbf{w}_{\text{tr}}[n]$), where $\mathbf{w}_{\text{tr}}[n]$ is the AWGN at the ith channel during the training phase. It is noteworthy that with MMSE channel estimation, the channel estimate and the channel estimation error remain uncorrelated (this happens due to the orthogonality principle [8]). In particular, we have that

$$\hat{\mathbf{h}}_i[n] = \mathbf{h}_i[n] + \tilde{\mathbf{h}}_i[n], \quad 1 \leq i \leq M, \tag{3}$$

where $\mathbf{h}_i \overset{\text{d}}{=} \mathcal{CN}(\mathbf{0}, (\beta_i - \hat{\beta}_i)\mathbf{I}_N)$ is the true channel fading of the ith transmitter (secondary or primary) and $\tilde{\mathbf{h}}_i \overset{\text{d}}{=} \mathcal{CN}(\mathbf{0}, \hat{\beta}_i\mathbf{I}_N)$ denotes its corresponding estimation error with $\hat{\beta}_i \triangleq \beta_i^2/(\sum_{j=1}^{M}\beta_j + N_0)$ [7, Eq. (12)].

Except the channel estimation errors, the channel aging effect occurs in several practical network setups. This is mainly because of the rapid channel variations during consecutive sample time instances, due to, e.g., user mobility and/or severe fast fading conditions. The popular autoregressive (Jakes) model of a certain order [9], based on the Gauss-Markov block fading channel, can accurately capture the latter effect. More specifically, it holds that

$$\hat{\mathbf{h}}_i[n] = \alpha^M \hat{\mathbf{h}}_i[n-M] + \sum_{m=0}^{M-1} \alpha^m \mathbf{e}_i[n-m], \tag{4}$$

where $\alpha \triangleq J_0(2\pi f_D T_s)$ with f_D and T_s denoting the maximum Doppler shift and the symbol sampling period, respectively. Moreover, $\mathbf{e}_i' \triangleq \sum_{m=0}^{M-1}\alpha^m \mathbf{e}_i[n-m]$ stands for the stationary Gaussian channel error vector due to the time variation of the channel, which is uncorrelated with $\mathbf{h}_i[n-M]$, while $\mathbf{e}_i' \overset{\text{d}}{=} \mathcal{CN}(\mathbf{0}, (1-\alpha^{2M})\beta_i\mathbf{I}_N)$. For the sake of mathematical simplicity and without loss of generality, we assume that the channel remains unchanged over the time period of training phase, while it may change during the subsequent data transmission phase. Thus, adopting the autoregressive model of order one, (4) simplifies to

$$\hat{\mathbf{h}}_i[n] = \alpha \hat{\mathbf{h}}_i[n-1] + \mathbf{e}_i[n]. \tag{5}$$

Substituting (3) into (5) and dropping from now on the time instance index n for ease of presentation (since all the involved random vectors are mutually independent), we have that

$$\hat{\mathbf{h}}_i = \alpha \mathbf{h}_i + \alpha\tilde{\mathbf{h}}_i + \mathbf{e}_i \triangleq \mathbf{g}_i + \boldsymbol{\epsilon}_i, \tag{6}$$

where $\mathbf{g}_i \overset{\text{d}}{=} \mathcal{CN}(\mathbf{0}, (\beta_i - \hat{\beta}_i)\alpha^2\mathbf{I}_N)$ and $\boldsymbol{\epsilon}_i \overset{\text{d}}{=} \mathcal{CN}(\mathbf{0}, \alpha^2\hat{\beta}_i + (1-\alpha^2)\beta_i)\mathbf{I}_N)$. It should be noted that the latter signal model in (6) combines both the channel aging effect and the channel estimation error. Hence, by defining $\mathbf{G} \triangleq [\mathbf{g}_1, \ldots, \mathbf{g}_{m_p}, \mathbf{g}_1, \ldots, \mathbf{g}_{m_c}]$ and $\mathbf{E} \triangleq [\boldsymbol{\epsilon}_1, \ldots, \boldsymbol{\epsilon}_{m_p}, \boldsymbol{\epsilon}_1, \ldots, \boldsymbol{\epsilon}_{m_c}]$, (1) can be reformulated as

$$\mathbf{y} = \mathbf{G}\mathbf{s} + \mathbf{E}\mathbf{s} + \mathbf{w}. \tag{7}$$

C. Data Transmission Phase: Signal Detection

Using the estimations of the channel gains of all transmitted signals from the training phase, the secondary receiver proceeds with the detection/decoding of the simultaneously transmitted streams from the m_c secondary transmitters. The mean-squared error (MSE) of the ith received data stream ($1 \leq i \leq m_c$) is formed as

$$\text{MSE}_i = \mathbb{E}\left[\left|s_i - \boldsymbol{\phi}_i^{\mathcal{H}}\mathbf{y}\right|^2\right], \tag{8}$$

where $\boldsymbol{\phi}_i$ denotes the MSE-optimal weight vector.

Corollary 1: The weight vector $\boldsymbol{\phi}_i$ that minimizes the MSE of the ith received stream is given by

$$\boldsymbol{\phi}_i = \sqrt{\beta_i}\left(\mathbf{C}\,\text{diag}\{\beta_j\}_{j=1}^{M}\mathbf{C}^{\mathcal{H}} + N_0\mathbf{I}_N\right)^{-1}\mathbf{c}_i, \tag{9}$$

where $\mathbf{C} \in \mathbb{C}^{N\times M}$ with $\mathbf{C} \overset{\text{d}}{=} \mathcal{CN}(\mathbf{0}, \mathbf{I}_N)$, and $\mathbf{c}_i$ represents its ith column vector.

Proof: The proof of (9) is relegated in Appendix A. ■

At the receiver, $\boldsymbol{\phi}_i^{\mathcal{H}}\mathbf{y}$ provides the detection/decoding of the ith transmitted stream, yielding

$$z_i = \boldsymbol{\phi}_i^{\mathcal{H}}\mathbf{y} = \boldsymbol{\phi}_i^{\mathcal{H}}\mathbf{g}_i s_i + \sum_{j\neq i}\boldsymbol{\phi}_i^{\mathcal{H}}\mathbf{g}_j s_j + \boldsymbol{\phi}_i^{\mathcal{H}}\mathbf{E}\mathbf{s} + \boldsymbol{\phi}_i^{\mathcal{H}}\mathbf{w}, \tag{10}$$

where $\mathbf{A} \triangleq \mathbf{C}\,\text{diag}\{\beta_j\}_{j=1}^{M}\mathbf{C}^{\mathcal{H}} + N_0\mathbf{I}_N$.

D. Spectrum Sensing

Let $\mathbf{r} \in \mathbb{C}^{N\times 1}$ represent the pre-processed received signal after removing the m_c secondary signals (i.e., after decoding them and removing their impact from the overall received signal). Then, starting from (7) yields

$$\mathbf{r} = \mathbf{G}_p\mathbf{s}_p + \mathbf{E}_p\mathbf{s}_p + \mathbf{w} = \mathbf{C}_p\,\text{diag}\{\sqrt{\beta_i}\}_{i=1}^{m_p}\mathbf{s}_p + \mathbf{w}, \tag{11}$$

where $\mathbf{G}_p \in \mathbb{C}^{N\times m_p}$, $\mathbf{E}_p \in \mathbb{C}^{N\times m_p}$, $\mathbf{C}_p \in \mathbb{C}^{N\times m_p}$, and $\mathbf{s}_p \in \mathbb{C}^{m_p\times 1}$ denote the true channel matrix, the estimation error matrix, the equivalent (joint) channel matrix, and the transmitted signals from the primary transmitters, respectively. For the distribution of the elements of $\mathbf{C}_p$ it holds $\mathbf{C}_p \overset{\text{d}}{=} \mathcal{CN}(\mathbf{0}, \mathbf{I}_N)$.

Using (11), the binary hypothesis test (energy detection (ED) of primary activity) is formulated as

$$T_{\text{ED}} \triangleq \sum_{l=0}^{L-1}\|\mathbf{r}(l)\|^2 \underset{\mathcal{H}_0}{\overset{\mathcal{H}_1}{\lessgtr}} \lambda, \tag{12}$$

where L and λ denote the number of samples for the received signal and the energy threshold, respectively, and

$$\begin{aligned} \mathcal{H}_0: &\quad \mathbb{E}[\mathbf{r}\mathbf{r}^{\mathcal{H}}] = N_0\mathbf{I}_N, \text{ no signal is present} \\ \mathcal{H}_1: &\quad \mathbb{E}[\mathbf{r}\mathbf{r}^{\mathcal{H}}] = \text{ any positive semi-definite matrix.} \end{aligned} \tag{13}$$

III. Performance Analysis

A. Detection Probability

We need to show that in the case of the $\mathcal{H}_1$ hypothesis, even if only the weakest signal is present, $T_{\text{ED}} > \lambda$ should hold. The latter condition can be modeled as

$$\mathbf{r}_{\min} = \sqrt{\beta_{\min}}\mathbf{c}_{\min}s_{\min} + \mathbf{w}, \tag{14}$$

where $\mathbf{r}_{\min}$ represents the remaining received signal, when only the primary transmitter experiencing the weakest channel gain (at the secondary receiver) is active. The transmitted

signal from the corresponding primary transmitter is defined as $s_{\min}$ with $\mathbb{E}[s_{\min}s_{\min}^{\mathcal{H}}] = \sigma_p^2$. Also, $\sqrt{\beta_{\min}}\mathbf{c}_{\min}$ satisfies that $\beta_{\min}\left\|\mathbf{c}_{\min}\right\|^2 = \min\{\beta_{\min}\left\|\mathbf{c}_{p,i}\right\|^2\}_{i=1}^{m_p}$, where $\mathbf{c}_{p,i}$ represents the ith column vector of $\mathbf{C}_p$. Notice that a Gaussian vector is isotropically distributed, i.e., it remains Gaussian distributed even if its norm is under some constraint [10, Theorem 1.5.5]. Thus, $\sqrt{\beta_{\min}}\mathbf{c}_{\min} \overset{\mathrm{d}}{=} \mathcal{CN}(\mathbf{0}, \beta_{\min}\mathbf{I}_N)$ and $\beta_{\min}\left\|\mathbf{c}_{\min}\right\|^2$ is the minimum of m_p non-identical χ^2_{2N} RVs.

Lemma 1: A closed-form expression for the PDF of $\mathcal{Y} \triangleq \beta_{\min}\left\|\mathbf{c}_{\min}\right\|^2$ is given by

$$f_{\mathcal{Y}}(x) = \sum_{s=1}^{m_p}\sum_{\substack{t_1=0\\t_1\neq t_s}}^{N-1}\cdots\sum_{\substack{t_{m_p}=0\\t_{m_p}\neq t_s}}^{N-1}\frac{\beta_1^{-t_1}\cdots\beta_s^{-N}\cdots\beta_{m_p}^{-t_{m_p}}}{t_1!\cdots t_{m_p}!\Gamma(N)} \times x^{\sum_{\substack{l=1\\l\neq s}}^{m_p} t_l+N-1}\exp\left(-\left(\sum_{t=1}^{m_p}\frac{1}{\beta_t}\right)x\right). \quad (15)$$

Proof: The CDF of $\mathcal{Y}$ stems as

$$\Pr[\mathcal{Y} < x] = 1 - \left(\prod_{t=1}^{m_p}\Pr[\beta_t\left\|\mathbf{c}_t\right\|^2 > x]\right). \quad (16)$$

Using the standard complementary CDF of a χ^2_{2N} RV into the previous expression, yields

$$F_{\mathcal{Y}}(x) = 1 - \prod_{t=1}^{m_p}\frac{\Gamma\left(N, \frac{x}{\beta_t}\right)}{\Gamma(N)}. \quad (17)$$

By differentiating (17), it holds that

$$f_{\mathcal{Y}}(x) = \sum_{s=1}^{m_p}\frac{x^{N-1}\exp\left(-\frac{x}{\beta_s}\right)}{\Gamma(N)\beta_s^N}\prod_{\substack{t=1\\t\neq s}}^{m_p}\frac{\Gamma\left(N, \frac{x}{\beta_t}\right)}{\Gamma(N)}. \quad (18)$$

Further, expanding $\Gamma(\cdot,\cdot)$ as a finite sum series according to [5, Eq. (8.352.4)], (15) is obtained. ∎

For our considered case of ED, the detection probability conditioned on $\mathcal{Y}$ is given by [11, Eq. (63)]

$$\Pr[T_{\text{ED}}|\mathcal{H}_1 > \lambda] = Q_{NL}\left(\sqrt{\frac{2L\sigma_p^2\mathcal{Y}}{N_0}}, \sqrt{\frac{\lambda}{N_0}}\right). \quad (19)$$

Corollary 2: The unconditional detection probability of the considered system with N receive antennas and m_p active primary transmitters is obtained in a closed form as

$$P_d(\lambda) = \sum_{s=1}^{m_p}\sum_{\substack{t_1=0\\t_1\neq t_s}}^{N-1}\cdots\sum_{\substack{t_{m_p}=0\\t_{m_p}\neq t_s}}^{N-1}\frac{\beta_1^{-t_1}\cdots\beta_s^{-N}\cdots\beta_{m_p}^{-t_{m_p}}}{t_1!\cdots t_{m_p}!\Gamma(N)} \times \mathcal{F}\left(\sum_{\substack{l=1\\l\neq s}}^{m_p} t_l + N, NL, \sqrt{\frac{2L\sigma_p^2}{N_0}}, \sqrt{\frac{\lambda}{N_0}}, \sum_{t=1}^{m_p}\frac{1}{\beta_t}\right), \quad (20)$$

where

$$\mathcal{F}(k,m,a,b,p) \triangleq \frac{\Gamma(k)\Gamma(m,\frac{b^2}{2})}{p^k\Gamma(m)} + \frac{a^2b^{2m}\Gamma(k)\exp\left(-\frac{b^2}{2}\right)}{m!p^k2^m(a^2+2p)} \times \sum_{l=0}^{k-1}\left(\frac{2p}{a^2+2p}\right)^l \underbrace{{}_1F_1\left(l+1, m+1; \frac{a^2b^2}{2a^2+4p}\right)}_{\mathcal{T}}. \quad (21)$$

Proof: Starting from (19) and using the PDF expression given by (15), integrals of the form [12, Eq. (1)] appear. Then, using the analytical solution [12, Eq. (12)] and after performing some straightforward manipulations, (20) arises. ∎

B. False Alarm Probability and Threshold Design

The false alarm probability with the ED given by (12) is defined as

$$P_f(\lambda) \triangleq \Pr[T_{\text{ED}}|\mathcal{H}_0 > \lambda]. \quad (22)$$

Under the $\mathcal{H}_0$ hypothesis, T_{ED} is the sum of the square ofs NL independent and identically distributed Gaussian RVs with zero mean and variance N_0, i.e, $T_{\text{ED}} \overset{\mathrm{d}}{=} N_0\chi^2_{2NL}$. Hence, using the standard complementary CDF of a chi-square RV, yields

$$P_f(\lambda) = \frac{\Gamma\left(NL, \frac{\lambda}{2N_0}\right)}{\Gamma(NL)}. \quad (23)$$

By inspecting (23), it becomes apparent that the false alarm probability is an *offline* operation, i.e., it is independent from the instantaneous channel gain and the number of primary signals. Thus, a convenient, yet effective strategy, to select the optimum energy threshold is by using (23). Doing so, it holds that

$$\lambda^* = P_f^{-1}(\tau), \quad (24)$$

where λ^* represents the optimum energy threshold (on the false alarm probability) for a predetermined target τ, while $P_f^{-1}(\cdot)$ denotes the inverse function of $P_f(\cdot)$, which can be efficiently calculated by using well-known inverse algorithms, e.g., [13]. In the sequel, the *online* detection probability can be directly computed by calculating $P_d(\lambda^*)$ using (20).

IV. Transmission Power of Secondary Nodes

We start by defining the transmission power of the secondary receiver in the case of the aforementioned signaling process (see II-A). Recall that in the case when the receiver senses the spectrum busy (idle) by a primary transmission, upon an ongoing secondary communication, then it immediately informs the secondary nodes to terminate (initiate) their transmissions using a certain probe message. In order not to cause an additional co-channel interference to the potentially active primary transmitter(s), the power used for this message is appropriately upper bounded. Particularly, it is defined as

$$p_R \triangleq \min\left\{p_{\max}, \frac{w_{\text{th}}}{Q_R}\right\}, \quad (25)$$

where $Q_R \triangleq \mathbb{E}[\max_i\{\left\|\mathbf{g}_i\right\|^2\}_{i=1}^{m_p}]$ and w_{th} denotes the outage power threshold of the primary service with regards to the secondary transmission(s), which is assumed as a predetermined parameter that is already known to all the secondary nodes.

Also, $p_{\max}$ denotes the maximum achievable (unconstrained) power of the overall secondary system.

Corollary 3: The transmission power at the receiver for the probe signal is expressed as

$$p_R = \left(\frac{1}{p_{\max}} + \frac{Q_R}{w_{\text{th}}} \right)^{-1}, \tag{26}$$

where Q_R is given in closed form as

$$Q_R = \sum_{i=1}^{m_p} \sum_{l=0}^{m_p} \frac{(-1)^l b_{R,i}^N}{l!\Gamma(N)} \underbrace{\sum_{n_1=1}^{m_p} \cdots \sum_{n_l=1}^{m_p}}_{n_1 \neq \cdots \neq n_l \cdots \neq l} \sum_{k_1=0}^{N-1} \cdots \sum_{k_l=0}^{N-1} \times \left(\prod_{t=1}^{l} \frac{b_{R,k_t}}{k_t!} \right) \frac{\Gamma\left(N + \sum_{t=1}^{l} k_t + 1\right)}{\left(b_{R,i} + \sum_{t=1}^{l} b_{R,n_t}\right)^{N+\sum_{t=1}^{l} k_t+1}}. \tag{27}$$

In (27), $b_{R,i} \triangleq (\beta_i - \hat{\beta}_i)\alpha^2$ is a certain parameter corresponding to the link between the secondary receiver and the ith primary transmitter ($1 \leq i \leq m_p$).

Proof: The proof is provided in Appendix B. ■

The transmission power for all the secondary transmitters can be obtained quite similarly. In particular, referring back to the structure of $\mathbf{H}_{\text{tr}} = [\mathbf{h}_1, \ldots, \mathbf{h}_{m_p}, \mathbf{h}_1, \ldots, \mathbf{h}_{m_c}]$ and $\mathbf{\Psi} = [\boldsymbol{\psi}_1, \ldots, \boldsymbol{\psi}_{m_p}, \boldsymbol{\psi}_1, \ldots, \boldsymbol{\psi}_{m_c}]$ from (2), each secondary transmitter sends its pilot in its corresponding symbol time duration. Notice that the pilots from primary transmitters are foregoing the ones of the secondary nodes. Hence, each secondary transmitter can capture its channel response with regards to every primary node, by monitoring the first m_p pilots during the training phase. Then, using MMSE channel estimation (as explicitly described earlier), the jth transmission power at the corresponding secondary node, p_j, is determined by

$$p_j = \left(\frac{1}{p_{\max}} + \frac{Q_j}{w_{\text{th}}} \right)^{-1}, \quad 1 \leq j \leq m_c, \tag{28}$$

where Q_j is directly obtained from (27), but denoting the jth secondary transmitter this time, instead of the secondary receiver. In the remaining symbol time duration of the training phase, where the secondary pilot symbol transmissions are sequentially established, $\{p_j\}_{j=1}^{m_c}$ are used to inform the secondary receiver about the corresponding channel states.

V. Performance Results and Discussion

We have numerically evaluated the performance expressions presented in Section III and cross compared the obtained results with equivalent ones obtained from Monte Carlo simulations. A perfect match between these evaluations and their respective simulation results was exhibited and, hence, the accuracy of the presented analysis was verified. Henceforth, for notational simplicity and without loss of generality, we assume a common path-loss exponent $\omega_i = 4 \ \forall \ i = 1, 2, \ldots, M$, corresponding to a classical macro-cell urban environment [14, Table 2.2], while we fix the probability of transmission for all the primary transmitters as $P_{\mathcal{A}}^p = 0.5$. Also, we set $\alpha = 0.1$, $\sigma_p^2 = 1$, and $p_{\max} = 20$dBm, while all the primary nodes use $p_{\max}$ for their transmissions.

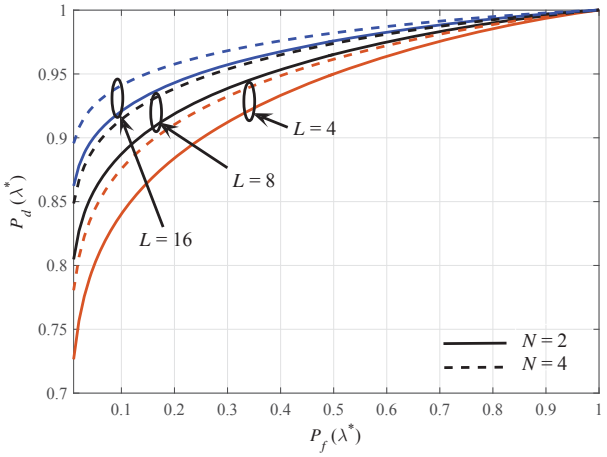

Fig. 1. Analytical ROC curve of the proposed approach for $m_p = 4$ with $d_1 = 0.31$, $d_2 = 0.1$, $d_3 = 0.15$, and $d_4 = 0.2$.

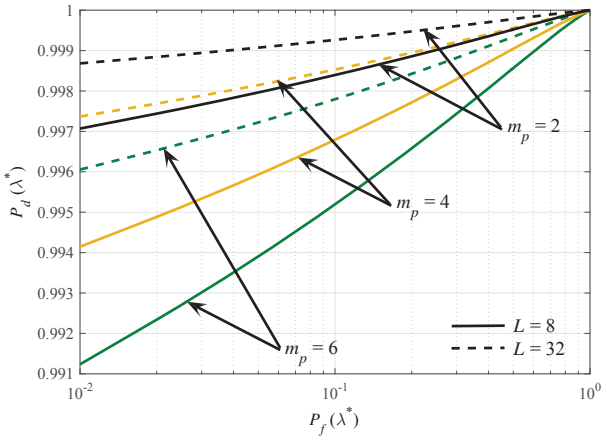

Fig. 2. Analytical ROC curve of the proposed approach for $N = 2$, various numbers of primary transmitters, and identical link distances with respect to the secondary receiver, i.e., $\{d_i\}_{i=1}^{m_p} = 0.1$.

By numerically evaluating (20), (23), and (24), Figs. 1 and 2 present the receive operating characteristics (ROC) curves for the scenario of non-identical and identical statistics, respectively. Obviously, the gap between the detection and false alarm probabilities increases as the number of antennas at the secondary receiver increase. This is further enhanced when the available number of samples increases. In addition, the presence of more primary transmitters degrades the detection performance, since adding more unknown primary signals increases their probability of being indistinguishable from noise. This behavior is in agreement with that in [15, Fig. 7]. It can be also seen from both figures that, the detection accuracy is reduced for far-distanced links, and this happens due to the unavoidable propagation attenuation on the received signals. In fact, severe channel fading due to propagation losses results to noise-like signals, hence, hardly indistinguishable.

APPENDIX

A. Derivation of (9)

Manipulating with (8) results in

$$\begin{aligned}\mathrm{MSE}_i &= \mathbb{E}\left[\left(s_i-\boldsymbol{\phi}_i^{\mathcal{H}}\mathbf{y}\right)\left(s_i-\boldsymbol{\phi}_i^{\mathcal{H}}\mathbf{y}\right)^{\mathcal{H}}\right]\\ &= 1+\boldsymbol{\phi}_i^{\mathcal{H}}\mathbf{A}\boldsymbol{\phi}_i - s_i\mathbf{y}^{\mathcal{H}}\boldsymbol{\phi}_i - \boldsymbol{\phi}_i^{\mathcal{H}}\mathbf{y}s_i^{\mathcal{H}}\\ &= 1+\left(\boldsymbol{\phi}_i^{\mathcal{H}}-(\mathbf{g}_i+\boldsymbol{\epsilon}_i)^{\mathcal{H}}\mathbf{A}^{-1}\right)\mathbf{A}\left(\boldsymbol{\phi}_i^{\mathcal{H}}-(\mathbf{g}_i+\boldsymbol{\epsilon}_i)^{\mathcal{H}}\mathbf{A}^{-1}\right)^{\mathcal{H}}\\ &\quad-(\mathbf{g}_i+\boldsymbol{\epsilon}_i)^{\mathcal{H}}\mathbf{A}^{-1}(\mathbf{g}_i+\boldsymbol{\epsilon}_i),\end{aligned} \tag{A.1}$$

where $\mathbf{A}\triangleq\mathbb{E}[\mathbf{y}\mathbf{y}^{\mathcal{H}}]=\mathbf{C}\,\mathrm{diag}\{\beta_j\}_{j=1}^{M}\mathbf{C}^{\mathcal{H}}+N_0\mathbf{I}_N$ represents the covariance matrix of the received signal. Since only the second term of (A.1) depends on $\boldsymbol{\phi}_i$, the optimal solution that minimizes MSE_i is $\boldsymbol{\phi}_i=\mathbf{A}^{-1}(\mathbf{g}_i+\boldsymbol{\epsilon}_i)$. Finally, noticing that $\mathbf{G}+\mathbf{E}=\mathbf{C}\,\mathrm{diag}\{\sqrt{\beta_j}\}_{j=1}^{M}$, (9) can be easily extracted.

B. Derivation of (26) and (27)

Regarding the derivation of (26) and recalling the Rayleigh fading environment, the PDF of the signal-to-noise ratio for the probe message transmitted from the secondary receiver becomes

$$f_{X_R}(x)=\begin{cases}\dfrac{N_0\exp\left(-\frac{N_0x}{p_{\max}\bar{X}_R}\right)}{p_{\max}\bar{X}_R}, & Q_R<\frac{w_{\mathrm{th}}}{p_{\max}},\\[2ex] \dfrac{N_0Q_R\exp\left(-\frac{N_0Q_Rx}{w_{\mathrm{th}}\bar{X}_R}\right)}{w_{\mathrm{th}}\bar{X}_R}, & Q_R>\frac{w_{\mathrm{th}}}{p_{\max}}.\end{cases} \tag{B.1}$$

where X_R and $\bar{X}_R$ denote the instantaneous and average input SNRs at the receiver. Hence, it yields that

$$\begin{aligned}F_{X_R}(x)&=1-\left(1-F_{X_R|p_{\max}}(x)\right)\left(1-F_{X_R|\frac{w_{\mathrm{th}}}{Q_R}}(x)\right)\\ &=1-\exp\left(-\frac{N_0\left(\frac{1}{p_{\max}}+\frac{Q_R}{w_{\mathrm{th}}}\right)x}{\bar{X}_R}\right).\end{aligned} \tag{B.2}$$

By differentiating (B.2), the corresponding PDF follows the classical exponential PDF with the yielded transmission power p_R as defined in (26).

Based on (7) and (11), we have that the actual channel matrix for the primary nodes can be expressed as $\mathbf{G}_p=\mathbf{C}_p\,\mathrm{diag}\{\sqrt{\beta_i}\}_{i=1}^{m_p}-\mathbf{E}_p$. Although the instantaneous values of $\mathbf{E}$ are not available, its distribution is known from (6), using MMSE channel estimation. It easily follows that

$$\mathbf{G}_p\overset{\mathrm{d}}{=}\mathbf{C}_p\,\mathrm{diag}\left\{\sqrt{(\beta_i-\hat{\beta}_i)\alpha^2}\right\}_{i=1}^{m_p}. \tag{B.3}$$

Thus, using the standard PDF/CDF expressions for chi-squared RVs, the maximum squared column norm of $\mathbf{G}_p$ is distributed as follows

$$\begin{aligned}f_{\max_i\{\|\mathbf{g}_i\|^2\}_{i=1}^{m_p}}(x)&=\sum_{i=1}^{m_p}f_{b_{R,i}\chi^2_{2N}}(x)\prod_{\substack{l=1\\l\neq i}}^{m_p}F_{b_{R,i}\chi^2_{2N}}(x)\\ &=\sum_{i=1}^{m_p}\frac{x^{N-1}\exp\left(-\frac{x}{b_{R,i}}\right)}{b_{R,i}^N\Gamma(N)}\\ &\quad\times\prod_{\substack{l=1\\l\neq i}}^{m_p}\left(1-\exp\left(-\frac{x}{b_{R,i}}\right)\sum_{k=0}^{N-1}\frac{\left(\frac{x}{b_{R,i}}\right)^k}{k!}\right).\end{aligned} \tag{B.4}$$

By utilizing the product expansion identities [16, Eq. (6)], (B.4) becomes after some simple manipulations

$$\begin{aligned}f_{\max_i\{\|\mathbf{g}_i\|^2\}_{i=1}^{m_p}}(x)&=\sum_{i=1}^{m_p}\sum_{l=0}^{m_p}\frac{(-1)^lb_{R,i}^N}{l!\Gamma(N)}\\ &\quad\times\underbrace{\sum_{n_1=1}^{m_p}\cdots\sum_{n_l=1}^{m_p}}_{n_1\neq\cdots\neq n_l\cdots\neq l}\sum_{k_1=0}^{N-1}\cdots\sum_{k_l=0}^{N-1}\left(\prod_{t=1}^{l}\frac{b_{R,k_t}}{k_t!}\right)\\ &\quad\times\exp\left(-\left(b_{R,i}+\sum_{t=1}^{l}b_{R,n_t}\right)x\right)x^{\sum_{t=1}^{l}k_t+N-1}.\end{aligned} \tag{B.5}$$

Thereby, recognizing that $Q=\int_0^\infty xf_{\max_i\{\|\mathbf{g}_i\|^2\}_{i=1}^{m_p}}(x)dx$ and utilizing [5, Eq. (3.381.4)], (27) is derived.

REFERENCES

[1] Y.-C. Liang, Y. Zeng, E. Peh, and A. T. Hoang, "Sensing-throughput tradeoff for cognitive radio networks," *IEEE Trans. Wireless Commun.*, vol. 7, no. 4, pp. 1326–1337, Apr. 2008.

[2] S. Song, K. Hamdi, and K. Letaief, "Spectrum sensing with active cognitive systems," *IEEE Trans. Wireless Commun.*, vol. 9, no. 6, pp. 1849–1854, Jun. 2010.

[3] S. Stotas and A. Nallanathan, "Overcoming the sensing-throughput tradeoff in cognitive radio networks," in *Proc. IEEE Int. Conf. Commun. (ICC)*, Cape Town, South Africa, May 2010, pp. 1–5.

[4] F. Moghimi, R. K. Mallik, and R. Schober, "Sensing time and power optimization in MIMO cognitive radio networks," *IEEE Trans. Wireless Commun.*, vol. 11, no. 9, pp. 3398–3408, Sep. 2012.

[5] I. S. Gradshteyn and I. M. Ryzhik, *Table of Integrals, Series, and Products*. Academic Press, 2007.

[6] J. I. Marcum, *Table of Q-functions*. U.S. Air Force Project RAND Res. Memo. M-339, ASTIA document AD 1165451, Santa Monica, CA, 1950.

[7] K. T. Truong and R. W. Heath, "Effects of channel aging in massive MIMO systems," *IEEE/KICS J. Commun. Netw.*, vol. 15, no. 4, pp. 338–351, Aug. 2013.

[8] S. M. Kay, *Fundamentals of statistical signal processing: Estimation theory*. Englewood Cliffs, NJ: Prentice Hall, 1993.

[9] K. E. Baddour and N. C. Beaulieu, "Autoregressive modeling for fading channel simulation," *IEEE Trans. Wireless Commun.*, vol. 4, no. 4, pp. 1650–1662, Jul. 2005.

[10] R. J. Muirhead, *Aspects of Multivariate Statistical Theory*. New York: Wiley Series in Probability and Statistics, 1982.

[11] P. Wang, J. Fang, N. Han, and H. Li, "Multiantenna-assisted spectrum sensing for cognitive radio," *IEEE Trans. Veh. Technol.*, vol. 59, no. 4, pp. 1791–1800, May 2010.

[12] P. C. Sofotasios, S. Muhaidat, G. K. Karagiannidis, and B. S. Sharif, "Solutions to integrals involving the Marcum Q-function and applications," *IEEE Signal Process. Lett.*, vol. 22, no. 10, pp. 1752–1756, Oct. 2015.

[13] A. R. DiDonato and A. H. Morris Jr., "Computation of the incomplete gamma function ratios and their inverse," *ACM Trans. Math. Software*, vol. 12, no. 4, pp. 377–393, Dec. 1986.

[14] A. J. Goldsmith, *Wireless Communications*. New York: Cambridge University Press, 2005.

[15] D. Morales-Jimenez, R. H. Y. Louie, M. R. McKay, and Y. Chen, "Analysis and design of multiple-antenna cognitive radios with multiple primary user signals," *IEEE Trans. Signal Process.*, vol. 63, no. 18, pp. 4925–4939, Sep. 2015.

[16] N. Miridakis, "Performance analysis of V-BLAST reception under multiuser decode-and-forward cooperation," *IET Commun.*, vol. 8, no. 6, pp. 899–904, Apr. 2014.